IJCRT.ORG ISSN : 2320-2882

INTERNATIONAL JOURNAL OF CREATIVE RESEARCH THOUGHTS (IJCRT)

An International Open Access, Peer-reviewed, Refereed Journal

Static Analysis of Multi-layered Smart Laminates in Cylindrical Bending

Sameer Sawarkar[1] and Sandeep Pendhari[2]

[1]Associate Professor, Pimpri Chinchwad College of Engineering & Research,
Ravet, Pune – 412101,

[2]Associate Professor, Veermata Jijabai Technological Institute,
Wadala, Mumbai – 400031,

Abstract

Displacement and stress analysis of a simply supported smart laminate (layered plate) under plane stress and plane strain conditions of elasticity has been performed with a new mixed Semi-analytical model. The displacements, transverse normal and shear stresses, electric potential and transverse electric displacement have been considered as primary variables. The mathematical model is a two-point boundary value problem (BVP) governed by set of coupled first ordered ordinary differential equations (ODEs). Accuracy and efficiency of the proposed model are assessed by comparing the numerical results obtained from the present investigation with available elasticity solutions.

Keywords: semi-analytical method, laminate, piezoelectricity, smart materials, plane stress, plane strain.

Introduction

In a piezoelectric material, the elastic and electric fields are reversibly coupled and this coupling effect is used in several engineering applications. The direct piezo-effect is used in sensors to infer the mechanical strain in material from induced electric potential. The inverse piezo-effect is used in actuators to control deformations due to static loads and vibrations due to dynamic loads, by applying appropriate electric potential difference. The combined use of sensing and actuating functions leads to development of a smart or intelligent material, which is a self-monitoring, self-controlling material. Use of smart materials is seen by and large in aircrafts and aerospace engineering.

Piezoelectricity was discovered in 1880. However, for a century, it remained to be just a scientific wonder. With the growth in aerospace projects, a need for self-governing materials for unmanned laboratories and unmanned ships grew. Exhaustive research on smart materials began in the decade of 1980. Since then, a substantial number of theories and analytical, numerical models have been reported for the analysis of smart materials. Ray et al. (1992, 1993) have presented three dimensional (3D) exact solutions for a single piezoelectric plate and 3D exact solutions for intelligent structure in cylindrical bending. Heyliger (1994) has obtained exact solution for unsymmetrical cross ply composite laminate attached with layers of piezoelectric material. Heyliger (1997) has also provided 3D exact solutions for single and two layers of piezoelectric materials. Exact solutions obtained by solving field equations are valuable because they represent near accurate response of the member. However, obtaining exact solutions for layered members with complex loading and boundary conditions becomes extremely difficult. Hence the researchers have focused their attention on approximate methods. Tiersten (1969), Lee and Moon (1989), Lee (1990), Dimitridis et al.

(1991), Crawley and Lazarus (1991), Wang and Rogers (1991) have presented analysis of smart materials using Classical plate theory (CPT). Chandrashekhara and Agarwal (1993), Jonnalagadda et al. (1994), Detwiler et al. (1995), Huang and Wu (1996), Bisegna et al. (2001), Vel and Batra (2001), Wu et al. (2004) have presented analytical models based upon First order shear deformation theory (FOST) and Ray et al. (1994), Kim et al. (1998) have used Higher order shear deformation theory (HOST) for analysis of smart materials.

In this paper, semi-analytical model developed by Kant et al. (2007) is reformulated for analysis of a smart laminate under mechanical and electrical load. A smart laminate under plane stress and plane strain conditions of elasticity is modeled as a mixed two-point BVP governed by a set of first ordered ODEs.

Mathematical Formulation

A smart laminate consisting of layers of isotropic/orthotropic substrate with piezoelectric material layers attached at top and bottom faces is considered. The plan dimensions of the laminate are $a \times b$ and thickness is h (Figure 1). A simple diaphragm support is assumed along the longitudinal edges, $x = 0, a$. Longitudinal edges of laminate are assumed to be grounded with zero potential. The laminate is subjected to transverse mechanical and/or electrical load with uniform intensity in y-direction. If $b << h$, the laminate is regarded to be in 2D plane stress condition of elasticity. If $b >> h$, the laminate is in 2D plane strain condition.

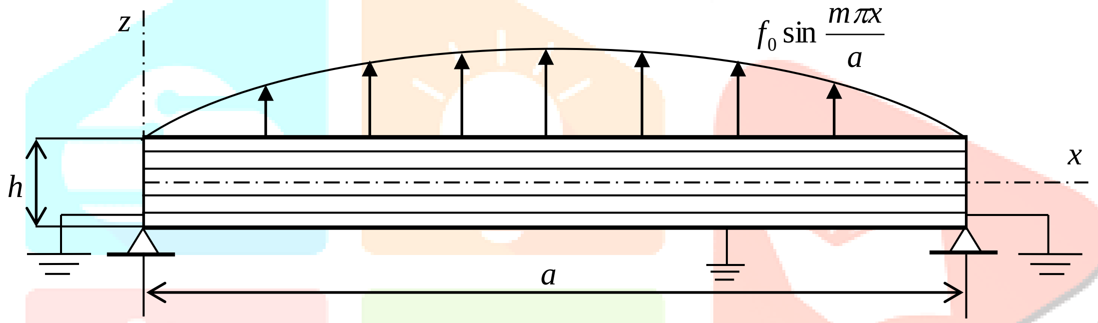

Figure 1: Smart laminate under mechanical and electric loading

The coupled elastic-electrical field equations in piezoelectric medium due to Tirsten (1969), 2D elasticity equilibrium equations, 2D strain-displacement relations and 2D charge equilibrium equation due to Maxwell (1865) are respectively given as;

$$\{\sigma\} = [C]\{\varepsilon\} - [e]\{E\}, \quad \{D\} = [e]^{\mathrm{T}}\{\varepsilon\} + [g]\{E\} \tag{1}$$

$$\frac{\partial \sigma_x}{\partial x} + \frac{\partial \tau_{xz}}{\partial z} + B_x = 0, \quad \frac{\partial \tau_{zx}}{\partial x} + \frac{\partial \sigma_z}{\partial z} + B_z = 0 \tag{2}$$

$$\varepsilon_x = \frac{\partial u}{\partial x}, \ \varepsilon_z = \frac{\partial w}{\partial z}, \ \gamma_{xz} = \frac{\partial u}{\partial z} + \frac{\partial w}{\partial x} \tag{3}$$

$$\frac{\partial D_x}{\partial x} + \frac{\partial D_z}{\partial z} = 0 \tag{4}$$

In these equations, stress vector $\{\sigma\}=\{\sigma_x, \sigma_x, \tau_{xz}\}^T$, strain vector $\{\varepsilon\}=\{\varepsilon_x, \varepsilon_z, \gamma_{xz}\}^T$, electric intensity vector $\{E\}=\{-\partial\phi/\partial x, 0, -\partial\phi/\partial z\}^T$, electric displacement vector $\{D\}=\{D_x, 0, D_z\}^T$ and B_x, B_z are body force intensities in x and y directions. The material coefficients matrix $[C]$, piezoelectric constants matrix $[e]$ due to Cady (1946) and dielectric constants matrix $[g]$ due to Tzau and Pandita (1987) for piezoelectric materials, which fall in the crystal group Rhombic, Class 7 are respectively;

$$[C]=\begin{bmatrix} C_{11} & C_{13} & 0 \\ C_{31} & C_{33} & 0 \\ 0 & 0 & C_{55} \end{bmatrix};\ [e]=\begin{bmatrix} 0 & 0 & e_{31} \\ 0 & 0 & e_{32} \\ 0 & 0 & e_{33} \\ 0 & e_{24} & 0 \\ e_{15} & 0 & 0 \\ 0 & 0 & 0 \end{bmatrix} \text{ and } [g]=\begin{bmatrix} g_{11} & 0 & 0 \\ 0 & g_{22} & 0 \\ 0 & 0 & g_{33} \end{bmatrix} \tag{5}$$

in which, the reduced material coefficients C_{ij} are for plane stress condition of elasticity are;

$$C_{11}=\frac{E_1}{1-\nu_{13}\nu_{31}};\ C_{13}=C_{31}=\frac{\nu_{13}E_1}{1-\nu_{13}\nu_{31}};\ C_{33}=\frac{E_3}{1-\nu_{13}\nu_{31}};\ C_{55}=G_{13} \tag{6}$$

and for plane strain condition of elasticity;

$$C_{11}=\frac{E_1(1-\nu_{23}\nu_{32})}{\Delta};\ C_{13}=C_{31}=\frac{E_1(\nu_{31}+\nu_{21}\nu_{32})}{\Delta};\ C_{33}=\frac{E_3(1-\nu_{12}\nu_{21})}{\Delta};\ C_{55}=G_{13} \tag{7}$$

where $\Delta=(1-\nu_{12}\nu_{21}-\nu_{23}\nu_{32}-\nu_{31}\nu_{13}-2\nu_{12}\nu_{23}\nu_{31})$

Equations (1)-(4) have a total of 11 unknowns u, w, ε_x, ε_z, γ_{xz}, σ_x, σ_z, τ_{xz}, D_x, D_z and ϕ in 11 equations. However, these unknowns are not entirely independent. After some algebraic manipulation of equations (1)-(4), a set of partial differential equations (PDEs) involving only six variables, called 'primary variables' u, w, σ_z, τ_{xz}, D_z and ϕ is obtained as below;

$$\begin{aligned}
\frac{\partial u}{\partial z} &= \frac{\tau_{xz}}{C_{55}}-\frac{e_{15}}{C_{55}}\frac{\partial\phi}{\partial x}-\frac{\partial w}{\partial x}\\
\frac{\partial w}{\partial z} &= \frac{g_{33}}{C_{33}g_{33}+e_{33}e_{33}}\sigma_z+\frac{e_{33}}{C_{33}g_{33}+e_{33}e_{33}}D_z-\frac{g_{33}C_{31}+e_{33}e_{31}}{C_{33}g_{33}+e_{33}e_{33}}\frac{\partial u}{\partial x}\\
\frac{\partial\phi}{\partial z} &= \frac{e_{33}}{C_{33}g_{33}+e_{33}e_{33}}\sigma_z-\frac{C_{33}}{C_{33}g_{33}+e_{33}e_{33}}D_z+\frac{C_{33}e_{31}-e_{33}C_{31}}{C_{33}g_{33}+e_{33}e_{33}}\frac{\partial u}{\partial x}\\
\frac{\partial\tau_{xz}}{\partial z} &= -\left[C_{11}-\frac{C_{13}g_{33}C_{31}+C_{13}e_{33}e_{31}}{C_{33}g_{33}+e_{33}e_{33}}+\frac{e_{31}C_{33}e_{31}-e_{31}e_{33}C_{31}}{C_{33}g_{33}+e_{33}e_{33}}\right]\frac{\partial^2 u}{\partial x^2}\\
&\quad -\left[\frac{C_{13}g_{33}+e_{31}e_{33}}{C_{33}g_{33}+e_{33}e_{33}}\right]\frac{\partial\sigma_z}{\partial x}-\left[\frac{C_{13}e_{33}-e_{31}C_{33}}{C_{33}g_{33}+e_{33}e_{33}}\right]\frac{\partial D_z}{\partial x}+B_x\\
\frac{\partial\sigma_z}{\partial z} &= -\frac{\partial\tau_{xz}}{\partial x}+B_z\\
\frac{\partial D_z}{\partial z} &= -\frac{e_{15}}{C_{55}}\frac{\partial\tau_{xz}}{\partial x}+\left(\frac{e_{15}e_{15}}{C_{55}}+g_{11}\right)\frac{\partial^2\phi}{\partial x^2}
\end{aligned} \tag{8}$$

To convert the PDEs in Equations (8) into ODEs, the displacement field, stress field, applied mechanical load and electrostatic potential are expressed in the form of single Fourier series satisfying the boundary conditions at $x = 0, a$ as;

$$\begin{Bmatrix} w(x,z) \\ \sigma_z(x,z) \\ D_z(x,z) \\ P(x,z) \\ \phi(x,z) \end{Bmatrix}=\sum_m \begin{Bmatrix} w_m(z) \\ \sigma_{zm}(z) \\ D_{zm}(z) \\ P_{0m}(z) \\ \phi_{0m}(z) \end{Bmatrix}\sin\alpha_m x,\ \begin{Bmatrix} u(x,z) \\ \tau_{xz}(x,z) \end{Bmatrix}=\sum_m \begin{Bmatrix} u_m(z) \\ \tau_{xzm}(z) \end{Bmatrix}\cos\alpha_m x;\ \text{where } \alpha_m=\frac{m\pi}{a} \tag{9}$$

Substituting Equations (9) and the derivatives into Equations (8), a set of first-ordered ODEs involving primary dependent variables u, w, σ_z, τ_{xz}, D_z and ϕ is obtained as;

$$\frac{du_m(z)}{dz} = -\alpha_m w_m(z) + \left(\frac{1}{C_{55}}\right)\tau_{xzm}(z) - \left(\frac{e_{15}}{C_{55}}\right)\alpha_m \phi_m(z)$$
$$\frac{dw_m(z)}{dz} = \left(\frac{g_{33}}{C_{33}g_{33}+e_{33}e_{33}}\right)\sigma_{zm}(z) + \left(\frac{e_{33}}{C_{33}g_{33}+e_{33}e_{33}}\right)D_{zm}(z) + \left(\frac{g_{33}C_{31}+e_{33}e_{31}}{C_{33}g_{33}+e_{33}e_{33}}\right)\alpha_m u_m(z)$$
$$\frac{d\phi_m(z)}{dz} = \left(\frac{e_{33}}{C_{33}g_{33}+e_{33}e_{33}}\right)\sigma_{zm}(z) - \left(\frac{C_{33}}{C_{33}g_{33}+e_{33}e_{33}}\right)D_{zm}(z) - \left(\frac{C_{33}e_{31}-e_{33}C_{31}}{C_{33}g_{33}+e_{33}e_{33}}\right)\alpha_m u_m(z)$$
$$\frac{d\tau_{xzm}(z)}{dz} = \left(C_{11} - \frac{C_{13}g_{33}C_{31}+C_{13}e_{33}e_{31}}{C_{33}g_{33}+e_{33}e_{33}} + \frac{e_{31}C_{33}e_{31}-e_{31}e_{33}C_{31}}{C_{33}g_{33}+e_{33}e_{33}}\right)\alpha_m^2 u_m(z)$$
$$-\left(\frac{C_{13}g_{33}+e_{31}e_{33}}{C_{33}g_{33}+e_{33}e_{33}}\right)\alpha_m \sigma_{zm}(z) - \left(\frac{C_{13}e_{33}-e_{31}C_{33}}{C_{33}g_{33}+e_{33}e_{33}}\right)\alpha_m D_{zm}(z) + B_x(x,z) \tag{10}$$
$$\frac{d\sigma_{zm}(z)}{dz} = \alpha_m \tau_{xzm}(z) + B_z(x,z)$$
$$\frac{dD_{zm}(z)}{dz} = \left(\frac{e_{15}}{C_{55}}\right)\alpha_m \tau_{xzm}(z) - \left(\frac{e_{15}e_{15}}{C_{55}} + g_{11}\right)\alpha_m^2 \phi_m(z)$$

The above Equations (10) represent the governing two-point BVP in ODEs in the domain $-h/2 \le z \le h/2$, with stress components known at the top and bottom surfaces of the laminate. Since the model developed is of mixed nature i.e. having both stress and displacement terms, the solution to Equations (10) is obtained using numerical integration. Change in material properties in case of a layered plate can be easily incorporated by changing the material properties matrices.

The secondary variables may be expressed in terms of primary variables as;

$$\sigma_x = \sum_m \left(-C_{11}\alpha_m u_m(z) + C_{13}\frac{dw_m}{dz} + e_{31}\frac{d\phi_m}{dz}\right)\sin\alpha_m x$$
$$D_x = \sum_m \left(e_{15}\frac{du_m(z)}{dz} + e_{15}\alpha_m w_m(z) - g_{11}\alpha_m \phi_m(z)\right)\cos\alpha_m x \tag{11}$$

Availability of efficient and accurate ODE numerical integrators for BVPs helps in computing reliable values of the primary and secondary variables.

Numerical Investigation and Discussion

Numerical investigation has been carried out on multi-layered smart beams and plates in cylindrical bending. The results obtained from present formulation have been compared with exact solutions available in the literature. Illustrative examples considered are discussed next.

Table 1: Material properties

Material	Properties
Graphite epoxy composite[a]	E_1 = 181 GPa, E_3 = 10.3 GPa, G_{13} = 7.17 GPa, ν_{13} = 0.28, e_{ij} = 0 g_{11} = 30.96E-12 F/m, g_{33} = 26.53E-12 F/m
PZT-5A[a]	E_1 = 61 GPa, E_3 = 53.2 GPa, G_{31} = 21.1 GPa, ν_{13} = 0.38 d_{13} = -171E-12 m/V, d_{33} = 374E-12 m/V, d_{15} = 584E-12 m/V g_{11} = 1.53E-8 F/m, g_{33} = 1.50E-8 F/m
PVDF[b]	E_1 = 23.2 GPa, E_3 = 10.5GPa, G_{13} = 2.55 GPa, ν_{13} = 0.177 e_{31} = -0.13 C/m^2, e_{33} = -0.28 C/m^2, e_{15} = -0.01 C/m^2, $\varepsilon_{11}/\varepsilon_0$ = 11.98, $\varepsilon_{33}/\varepsilon_0$ = 11.98
PZT-4[c]	E_1 = 81.3 GPa, E_3 = 64.5 GPa, G_{13} = 25.6 GPa, ν_{13} = 0.432

e_{31} = -5.20 C/m^2, e_{33} = 15.08 C/m^2, e_{15} = 12.72 C/m^2
$\varepsilon_{11}/\varepsilon_0$ = 1475, $\varepsilon_{33}/\varepsilon_0$ = 1300

[a] Kapuria (2001), [b] Heylinger and Brooks (1996), [c] Lu et al. (2005)

Example 1

A simply supported layered smart beam with substrate of graphite epoxy composite bonded with a piezoelectric layer of PZT-5A at its top surface is considered. All the laminae of substrate have equal thickness and the ratio of piezoelectric layer thickness to the laminate thickness is *0.1*. The interface of PZT-5A layer with substrate is grounded to zero potential (Figure 2).

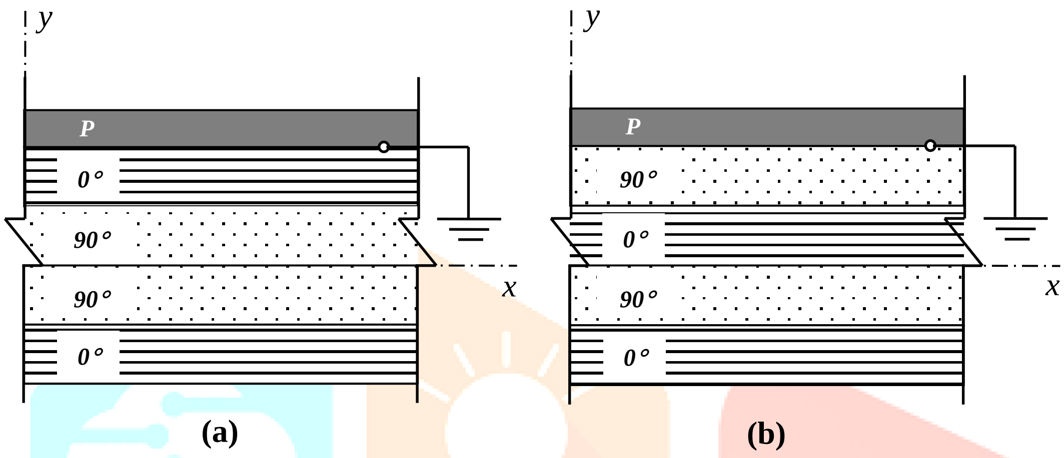

Figure 2: Stacking in laminated smart beam (a) symmetric, (b) asymmetric

Properties of the graphite epoxy composite and PZT-5A are given in Table 1. The smart beam is referred to as a *sensory beam* when subjected to transverse mechanical load and as an *actuating beam* when subjected to electric potential load. The sensory beam is subjected to a sinusoidal traction at top surface, $P = p_0 \sin\frac{\pi x}{a}$ with $p_0 = 1$ and the actuating beam is subjected to a sinusoidal potential at top surface, $\phi = \phi_0 \sin\frac{\pi x}{a}$ with $\phi_0 = 1$.

Three kinds of beam, viz. thick beam (*s* = *a/h* = *4*), moderately thick beam (*s* = *10*) and slender beam (*s* = *100*) have been investigated.

Results are non-dimensionalised for the sensory beam as;

$$\bar{u} = \frac{100E_2(u)}{hs^3 p_0}, \bar{w} = \frac{100E_2(w)}{hs^4 p_0}, \bar{\sigma}_x, = \frac{(\sigma_x)}{s^2 p_0}, \bar{\tau}_{xz} = \frac{(\tau_{xz})}{sp_0}, \bar{D}_z = \frac{D_z}{d_T p_0}$$

and for the actuating beam as;

$$\bar{u} = \frac{10E_2(u)}{d_T s\phi_0}, \bar{w} = \frac{10E_2(w)}{d_T s^2\phi_0}, \bar{\sigma}_x = \frac{h(\sigma_x)}{10E_2 d_T\phi_0}, \bar{\tau}_{xz} = \frac{sh(\tau_{xz})}{E_2 d_T\phi_0}, \bar{D}_z = \frac{D_z h}{100E_2 d_T^2\phi_0}$$

in which, $d_T = 374\times10^{-12}$ *C/N*.

Following lamination orders are considered for sensory and actuating beams. Orientation of fibers is given relative to *x*-direction.

1. Symmetric substrate laminate with PZT-5A layer bonded at top [*p*/0°/90°/90°/0°]

2. Asymmetric substrate laminate with PZT-5A layer bonded at top [*p*/0°/90°/0°/90°];

where alphabet *p* represents a piezoelectric layer.

Results obtained using present formulation are compared with the exact solutions given by Kapuria (2001). The results are presented in Table 2 for sensory beam and Table 3 for actuating beam. Through thickness variations in normalized in-plane displacement, normalized in-plane normal stress and normalized transverse shear stress are shown in Figures 3-5, which show that the present model is precisely capturing slope discontinuities in u, σ_x and τ_{xz} at the interface. The non-linearity of in-plane displacement u is much pronounced in a thick beam ($s = 4$) compared to that in a moderately thick beam ($s = 10$). Actuating voltage is observed to create large inter-laminar in-plane normal stresses σ_x.

Example 2

A simply supported symmetric 3-layer cross-ply [$90°/0°/90°$] layered plate of PVDF (material properties given in Table 1) in cylindrical bending is investigated. The plate is subjected to two loading cases; a *sensory* plate subjected to sinusoidal mechanical load with maximum intensity $p_0 = 1$ and an *actuating* plate subjected to sinusoidal electric load with maximum intensity $\phi_0 = 1$. Two aspect ratios, $a/h = 4, 100$ are considered for investigation. Results obtained by present formulation are compared with exact solutions given by Heylinger and Brooks (1996). The results for both the cases are presented in Figures 6 to 9. A prominent non-linear variation in each layer is seen in in-plane displacement u, in-plane normal stress σ_x and transverse shear stress τ_{xz} in a thick plate ($s = 4$) in Figures 6-8. These variations approach linearity in layer for a slender plate ($s = 100$).

Example 3

A simply supported 2-ply bimorph [*PZT-4/PVDF*] plate with equal layer thicknesses in cylindrical bending is investigated. Material properties are given in Table 1. Thickness of each layer is assumed to be *0.005 m*. The plate is subjected to two loading cases; a *sensory* plate subjected to sinusoidal mechanical load and an *actuating* plate subjected to sinusoidal electric load, both with unit maximum intensities. Several aspect ratios, $a/h = 2, 6, 10, 20, 50, 100$ are considered for investigation. Numerical values of stresses and displacements at critical points are reported in Table 4 for sensory plate and in Table 5 for actuating plate, which, in absence of similar data, may serve as benchmark results.

Example 4

To further assess the virtuosity of the present model, a *PZT-4* based piezoelectric functionally graded material (PFGM) plate in cylindrical bending is analyzed. Geometry of the plate is assumed as $a = h = 1m$. Material elastic and electric properties are assumed to vary in the thickness direction according to exponential law; $C_{ij} = C_{ij}^0 e^{\beta z}$, $e_{ij} = e_{ij}^0 e^{\beta z}$, $g_{ij} = g_{ij}^0 e^{\beta z}$, where superscript (^{0}) indicates value of the quantity at the base ($h = 0$) and β is a constant indicating gradient in z direction. Material properties are given in Table 1. Three different gradiemts are investigated, viz. $\beta = -1, 0, 1$ with $\beta = 0$ indicating homogeneous piezo-material. The plate is subjected to transverse mechanical load $P = p_0 \sin\frac{\pi x}{a}$ with $p_0 = 1$ and electric potential $\phi = \phi_0 \sin\frac{\pi x}{a}$ with $\phi_0 = 1$ at top surface. Results obtained for through-thickness variations in mechanical and electric quantities at a section $x = 0.25a$ are compared with exact results given by Lu et.al. (2005). Results for mechanical loading are given in Figure 10 and for electrical loading are given in Figure 11, which show that change in material gradient index β of PFMG hardly affects the displacements whereas it largely affects the stresses.

Concluding remarks

A new Semi-analytical methodology for the analysis of a smart laminate under plane stress and plane strain conditions of elasticity has been described in this paper. The mathematical model is highly accurate and computationally inexpensive. The methodology is free from any simplifying assumptions in thickness direction. The stresses and displacements are found simultaneously and with the same degree of accuracy, which is a unique feature of this model. Accuracy of the formulation is ascertained in numerical investigation by comparing the results obtained using present formulation with available exact solutions and are found to be in very good agreement with the same. The model is versatile and performs equally efficiently for a layered smart beam, for a piezoelectric cross-ply and for a PFGM plate too. Additional results for a bimorph have been reported for future reference.

References

1. Bisegna P, Caruso G and Maceri F (2001) A layer-wise Reissner-Mindlin type model for the vibration analysis and suppression of piezo-actuated plates. *Computers and Structures* 79(26-28): 2309-2319.
2. Cady W.G. 1946, “Piezoelectricity”, *Volumes I & II, Dover Publications, New York.*
3. Chandrashekhara K and Agarwal AN (1993) Active vibration control of laminated composite plates using piezoelectric devices: a finite element approach. *Journal of Intelligent Materials Systems and Structures* 4: 496-508.
4. Crawley EF and Lazarus KB (1991) Induced strain actuation of isotropic and anisotropic plates. *AIAA Journal* 29: 944-951.
5. Detwiler DT, Shen MH and Venkayya VB (1995) Finite element analysis of laminated composite structures containing distributed piezoelectric actuators and sensors. *Finite Elements in Analysis and Design* 20(2): 87-100.
6. Dimitridis EK, Fuller CR and Roger CA (1991) Piezoelectric actuators for distributed vibration excitation of thin plates *Journal of Vibration and Acoustics, Transactions of the ASME*, 113: 100-107.
7. Heyliger P (1994) Static behavior of laminated piezoelectric elastic plates. *AIAA Journal*, 32(12): 2481-2484.
8. Heyliger P (1997) Exact solutions for simply supported laminated piezoelectric plates. *Journal of Applied Mechanics* 64: 299-306.
9. Heylinger P and Brooks S (1996) Exact solutions for laminated piezoelectric plates in cylindrical bending. *Journal of Applied Mechanics* 63: 903-910.
10. Huang JH and Wu TL (1996) Analysis of hybrid multi-layered piezoelectric plates. *International Journal of Engineering Science* 34(2): 171-181.
11. Jonnalagadda KD, Blandford GE and Tauchert TR (1994) Piezo-thermo-elastic composite plate analysis using first ordered shear deformation theory. *Computers and Structures* 51: 79-89.
12. Kant T, Pendhari S and Desai Y (2007) On Accurate Stress Analysis of Composite and Sandwich Narrow Beams. *International Journal for Computational Methods in Engineering Science and Mechanics* 8(165): 165-177.
13. Kapuria S (2001) An efficient coupled theory for multilayered beams with embedded piezoelectric sensory and active layers. *International Journal of Solids and Structures* 38: 9179-9199.
14. Kim J, Varadan, VV and Varadan VK (1998) Finite element modeling of structures including piezoelectric active devices. *Journal of Intelligent Material Systems and Structures* 40(5): 817-832.
15. Lee CK and Moon FC (1989) Laminated piezo-polymer plates for torsion and bending sensors and actuators. *Journal of the Acoustical Society of America* 85: 2432-2439.
16. Lee CK (1990) Theory of laminated piezoelectric plates for the design of distributed sensors/actuators, Part I: Governing equations and reciprocal relationships. *Journal of Acoustical Society of America* 87: 1144-1158.
17. Lu P Lee HP and Lu C (2005) An exact solution for functionally graded piezoelectric laminates in cylindrical bending. *International Journal of Mechanical Sciences* 47: 437-458.

18. Maxwell JC (1865) A dynamical theory of the electromagnetic field. *Royal Society Transactions* 155: 459-512.
19. Ray MC, Bhattacharyya R and Samanta B (1994) Static analysis of an intelligent structure by the finite element method. *Computers & Structures* 52(4): 617-631.
20. Ray MC, Rao KM And Samanta B (1992) Exact analysis of coupled electro-elastic behavior of a piezoelectric plate under cylindrical bending. *Computers and Structures* 45(4): 667-677.
21. Ray MC, Rao KM and Samanta B (1993) Exact solution for static analysis of an Intelligent structure under cylindrical bending. *Computers and Structures* 47(6): 1031-1042.
22. Tiersten HF (1969), "Linear piezoelectric plate vibrations", *Plenum, New York*.
23. Tzau HS and Pandita S (1987) A multipurpose dynamic and tactile sensor for robot manipulators. *Journal of Robot Systems* 4: 719-741.
24. Vel SS and Batra RC (2001) Generalized plane strain thermo-elastic deformation of laminated anisotropic thick plates. *International Journal of Solids and Structures* 38: 1395-1414.
25. Wang BT and Rogers CA (1991) Laminate plate theory for spatially distributed strain actuators. *Journal of Composite Materials* 25: 433-452.
26. Wu L, Jiang Z and Feng W (2004) An analytical solution for static analysis of a simply supported moderately thick sandwich piezoelectric plate. *Structural Engineering and Mechanics* 17(5): 641-654.

Table 2: Normalized displacements and stresses in a sensory beam

Beam Type	a/h	Source	$\bar{u}$ *(0, h/2)*	$\bar{w}$ *(a/2, 0)*	$\bar{\sigma}_x$ *(a/2, h/2)*	$\bar{\sigma}_x$ *(a/2, 0.4h)*	$\bar{\tau}_{xz}$ *(0, 0.4h)*
Symmetric Beam	4	Exact[a]	2.478	-3.063	-0.514	-0.847	-0.406
		Present	2.494	-3.073	-0.511	-0.853	-0.407
		% Error	0.637	0.332	-0.486	0.648	0.283
	10	Exact[a]	1.679	-1.297	-0.34	-0.706	-0.434
		Present	1.703	-1.305	-0.331	-0.718	-0.435
		% Error	1.434	0.674	-2.728	1.726	0.218
	100	Exact[a]	1.521	-0.944	-0.306	-0.676	-0.44
		Present	1.543	-0.952	-0.295	-0.687	-0.441
		% Error	1.393	0.889	-3.683	1.641	0.227
Asymmetric Beam	4	Exact[a]	3.2611	-4.0352	-0.6718	-1.1177	-0.5373
		Present	3.2994	-4.0707	-0.6697	-1.1328	-0.537
		% Error	1.174	0.879	-0.312	1.35	-0.055
	10	Exact[a]	2.5113	-2.1656	-0.5086	-1.0157	-0.5794
		Present	2.5515	-2.187	-0.497	-1.0361	-0.5812
		% Error	1.6	0.988	-2.28	2.008	0.31
	100	Exact[a]	2.361	-1.7873	-0.476	-0.9935	-0.5886
		Present	2.3992	-1.8076	-0.4622	-1.0124	-0.5908
		% Error	1.617	1.135	-2.89	1.902	0.373

[a] Kapuria (2001)

Table 3: Normalized displacements and stresses in an actuating beam

Beam Type	a/h	Source	$\bar{u}$ *(0, h/2)*	$\bar{w}$ *(a/2, 0)*	$\bar{\sigma}_x$ *(a/2, h/2)*	$\bar{\sigma}_x$ *(a/2, 0.4h)*	$\bar{\tau}_{xz}$ *(0, 0.4h)*	$\bar{D}_z$ *(a/2, h/2)*
Symmetric Beam	4	Exact[a]	-3.638	1.737	-2.032	1.617	-6.583	-1.512
		Present	-3.606	1.74	-2.031	1.576	-6.604	-1.517
		% Error	-0.879	0.181	-0.027	-2.517	0.334	0.368
	10	Exact[a]	-3.017	1.2837	-2.144	1.429	-6.868	-1.505
		Present	-3.016	1.285	-2.142	1.413	-6.885	-1.501
		% Error	-0.006	0.159	-0.07	-1.064	0.259	-0.23
	100	Exact[a]	-2.89	1.1866	-2.167	1.389	-6.927	-1.504
		Present	-2.894	1.188	-2.165	1.391	-6.944	-1.498
		% Error	0.145	0.147	-0.06	0.147	0.253	-0.393
Asymmetric Beam	4	Exact[a]	-4.022	2.2938	-1.959	1.734	-6.409	-1.515
		Present	-3.9893	2.3002	-1.9552	1.69445	-6.4312	-1.526
		% Error	-0.812	0.279	-0.19	-2.28	0.346	0.731
	10	Exact[a]	-3.47	1.8887	-2.058	1.574	-6.409	-1.508
		Present	-3.4697	1.8916	-2.0528	1.55989	-6.6764	-1.5116

	% Error	-0.006	0.153	-0.249	-0.895	4.172	0.242
100	Exact[a]	-3.557	1.801	-2.079	1.541	-6.71	-1.507
	Present	-3.362	1.804	-2.073	1.5431	-6.7271	-1.508
	% Error	-5.463	0.167	-0.284	0.136	0.255	0.112

[a] Kapuria (2001)

Table 4: Displacement and stress values in a sensory bimorph [*PZT4/PVDF*] plate

Parameter (Position)	Aspect ratio *a/h*					
	2	*6*	*10*	*20*	*50*	*100*
u (0, h/2)	-0.3282E-12	-0.6792E-11	-0.2998E-10	-0.2345E-9	-0.364E-8	-0.2909E-7
u (0, 0)	0.2789E-12	0.3787E-11	0.1524E-10	0.1136E-9	0.1738E-8	0.1386E-7
u (0, -h/2)	0.3154E-12	0.1157E-10	0.5555E-10	0.4517E-9	0.7090E-8	0.5676E-7
w (0, h/2)	0.9827E-12	0.4182E-10	0.2916E-9	0.4447E-8	0.1713E-6	0.2735E-5
w (0, 0)	0.9582E-12	0.4198E-10	0.2922E-9	0.4449E-8	0.1713E-6	0.2735E-5
w (0, -h/2)	0.8909E-12	0.4156E-10	0.2911E-9	0.4445E-8	0.1713E-6	0.2735E-5
σ_x *(0, h/2)*	5.8033	38.485	101.59	396.7	2.4619E3	9.8377E3
σ_x *(0, 0)*	-4.429	-20.15	-49.43	-187.6	-1.162E3	-4.655E3
σ_x *(0, 0)*	-0.909	-4.149	-10.32	-39.8	-0.249E3	-1.002E3
σ_x *(0, -h/2)*	-1.155	-14.11	-40.65	-165.3	-1.038E3	-4.154E3
σ_z *(0, 0)*	0.2307	0.3558	0.3728	0.3806	0.3828	0.3831
τ_{xz} *(0, 0)*	0.5667	2.3054	3.9751	8.0703	20.262	40.549
ϕ *(0, 0)*	0.2909E-4	0.4406E-3	0.0013	0.0054	0.0337	0.1351
D_z *(0, h/2)*	0.2338E-9	0.2122E-9	0.2495E-9	0.4531E-9	0.1899E-8	0.7068E-8
D_z *(0, 0)*	-9E-13	0.0193E-9	0.0632E-9	0.2698E-9	0.1717E-8	0.6885E-8
D_z *(0, -h/2)*	0.6123E-12	0.2152E-10	0.6547E-10	0.2721E-9	0.1719E-8	0.6888E-8

Table 5: Displacement and stress values in an actuating bimorph [*PZT4/PVDF*] plate

Parameter (Position)	Aspect ratio *a/h*					
	2	*6*	*10*	*20*	*50*	*100*
u (0, h/2)	-0.1451E-9	-0.6499E-10	-0.4208E-10	-0.2592E-10	-0.2337E-10	-0.0348E-9
u (0, 0)	0.1805E-10	0.0719E-10	-0.0383E-10	-0.2261E-10	-0.0675E-9	-0.1381E-9
u (0, -h/2)	-0.5276E-10	-0.4459E-10	-0.4372E-10	-0.5922E-10	-0.1276E-9	-0.2493E-9
w (0, h/2)	-0.2338E-9	-0.2122E-9	-0.2495E-9	-0.4531E-9	-0.1899E-8	-0.7068E-8
w (0, 0)	-0.1653E-9	-0.2012E-9	-0.2444E-9	-0.4505E-9	-0.1897E-8	-0.7066E-8
w (0, -h/2)	-0.1776E-9	-0.2252E-9	-0.2693E-9	-0.4758E-9	-0.1923E-8	-0.7091E-8
σ_x *(0, h/2)*	302.29	56.179	12.825	-7.5062	-13.437	-14.293
σ_x *(0, 0)*	-338.13	-65.634	-11.882	13.335	20.636	21.672
σ_x *(0, 0)*	-86.005	-26.558	-14.932	-9.5122	-7.957	-7.74
σ_x *(0, -h/2)*	181.73	37.481	14.494	3.9111	0.8462	0.4046
σ_z *(0, 0)*	-22.062	-0.5259	-0.0556	0.0019	0.001	0.2856
τ_{xz} *(0, 0)*	-24.507	-1.2623	0.0602	0.2237	0.1122	0.0577
ϕ *(0, 0)*	0.7099	0.9528	0.9782	0.9894	0.9925	0.993
D_z *(0, h/2)*	-0.1939E-5	-0.2795E-6	-0.1167E-6	-0.4629E-7	-0.2637E-7	-0.2352E-7
D_z *(0, 0)*	-0.0019E-5	-0.0221E-6	-0.0224E-6	-0.2253E-7	-0.2256E-7	-0.2257E-7
D_z *(0, -h/2)*	-0.1465E-7	-0.2145E-7	-0.2216E-7	-0.2246E-7	-0.2255E-7	-0.2256E-7

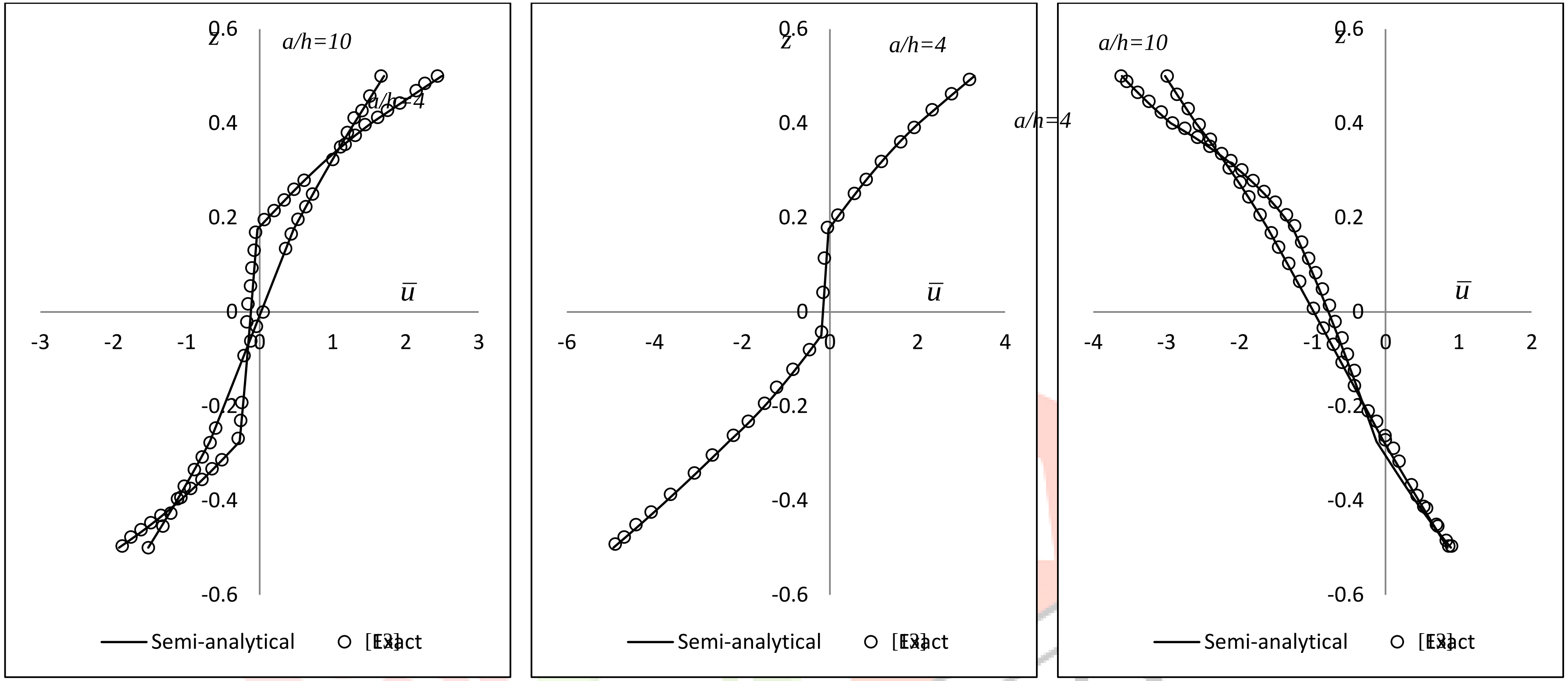

(a) **(b)** **(c)**

Figure 3: Through thickness variation of normalized in-plane displacement in smart beam
(a) symmetric sensory, (b) asymmetric sensory, (c) symmetric actuating

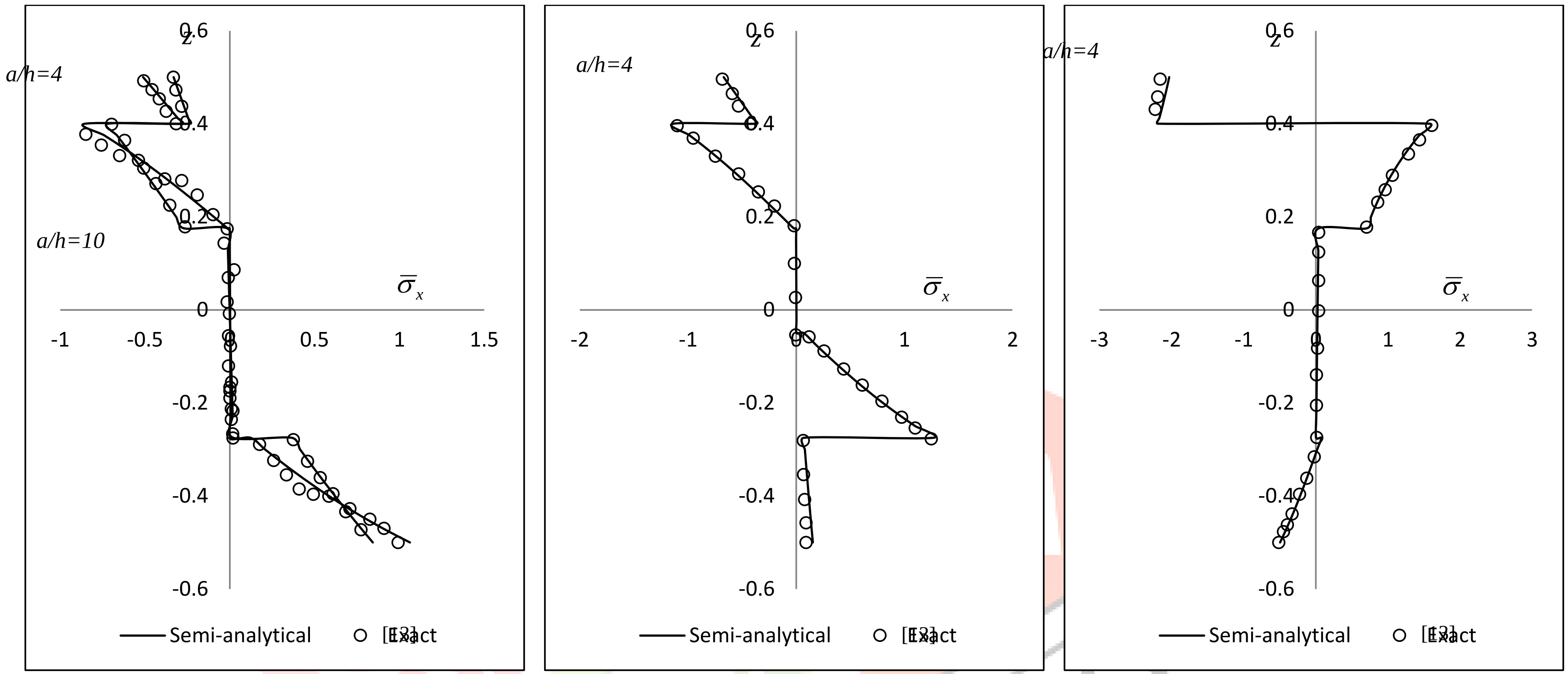

(a) **(b)** **(c)**

Figure 4: Through thickness variation of normalized in-plane normal stress in smart beam
(a) symmetric sensory, (b) asymmetric sensory, (c) symmetric actuating

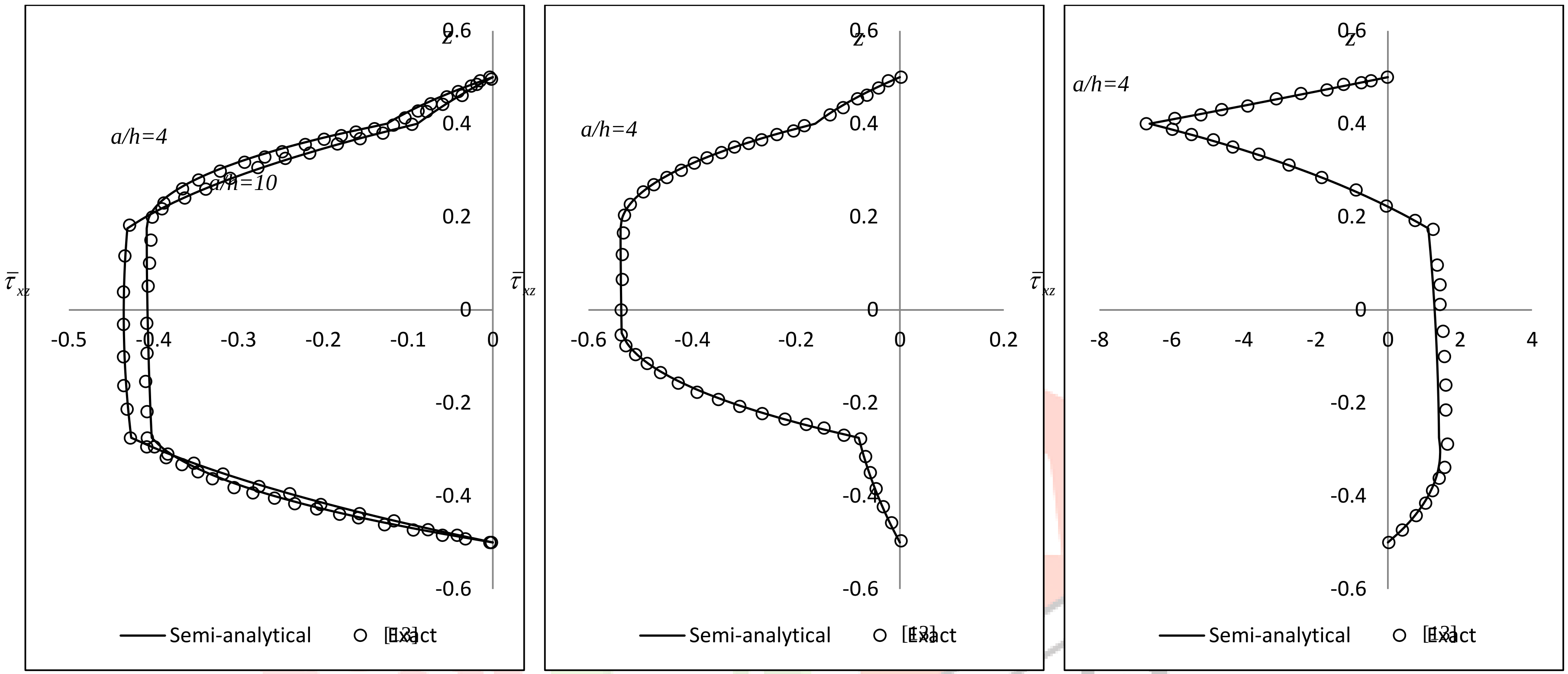

(a) **(b)** **(c)**

Figure 5: Through thickness variation of normalized transverse shear stress in smart beam
(a) symmetric sensory, (b) asymmetric sensory, (c) symmetric actuating

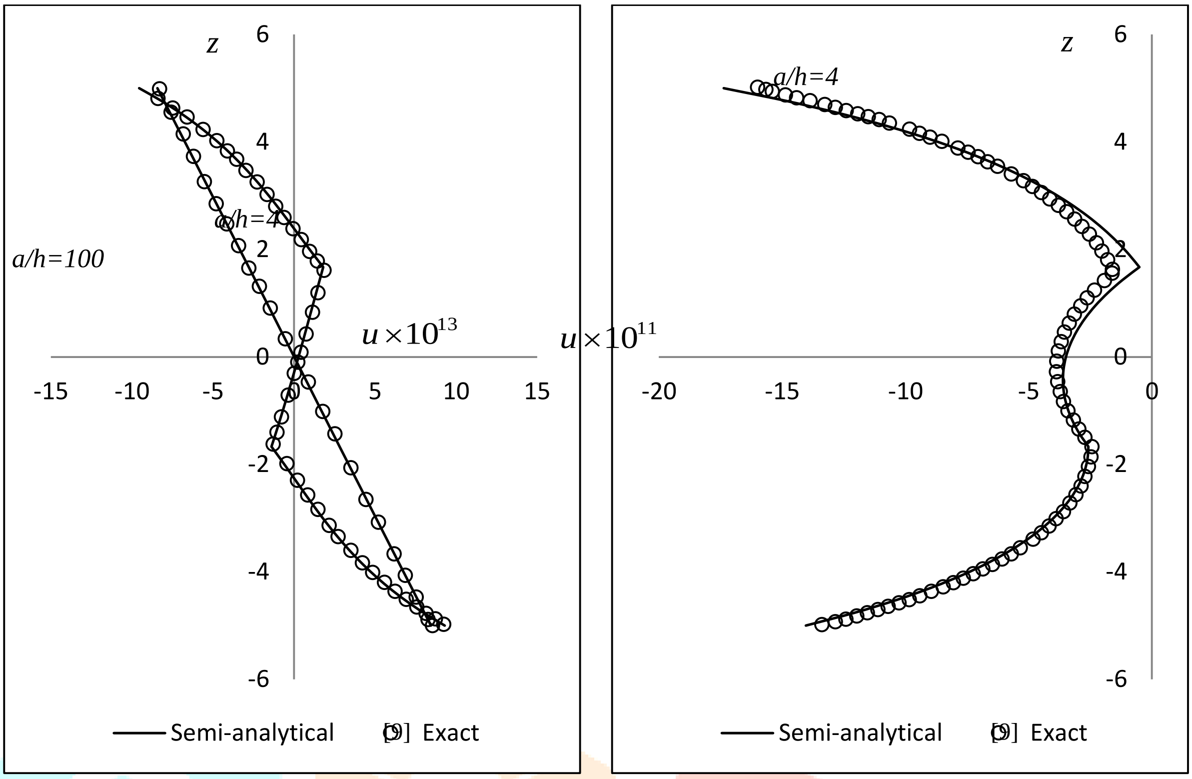

(a) (b)

Figure 6: Through thickness variation of in-plane displacement in PVDF cross ply laminate for (a) applied load case, (b) applied electric potential case

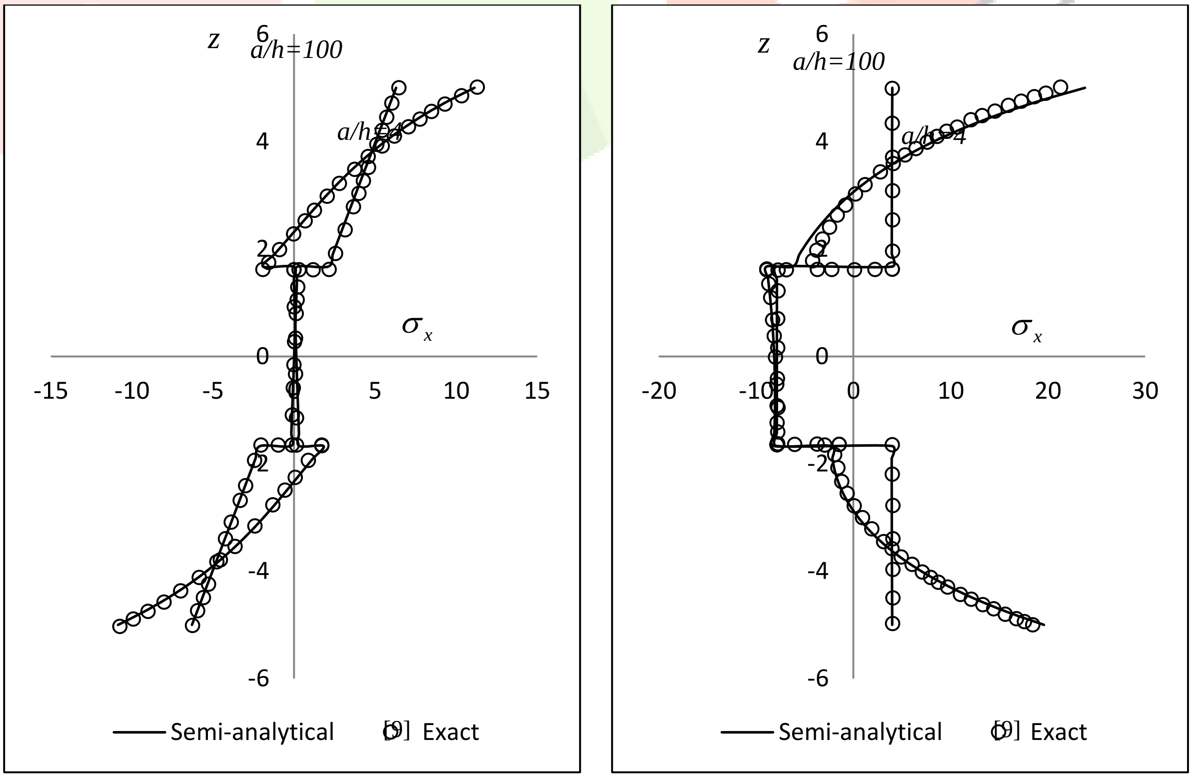

(a) (b)

Figure 7: Through thickness variation of in-plane normal stress in PVDF cross ply laminate (a) applied load case, (b) applied electric potential case

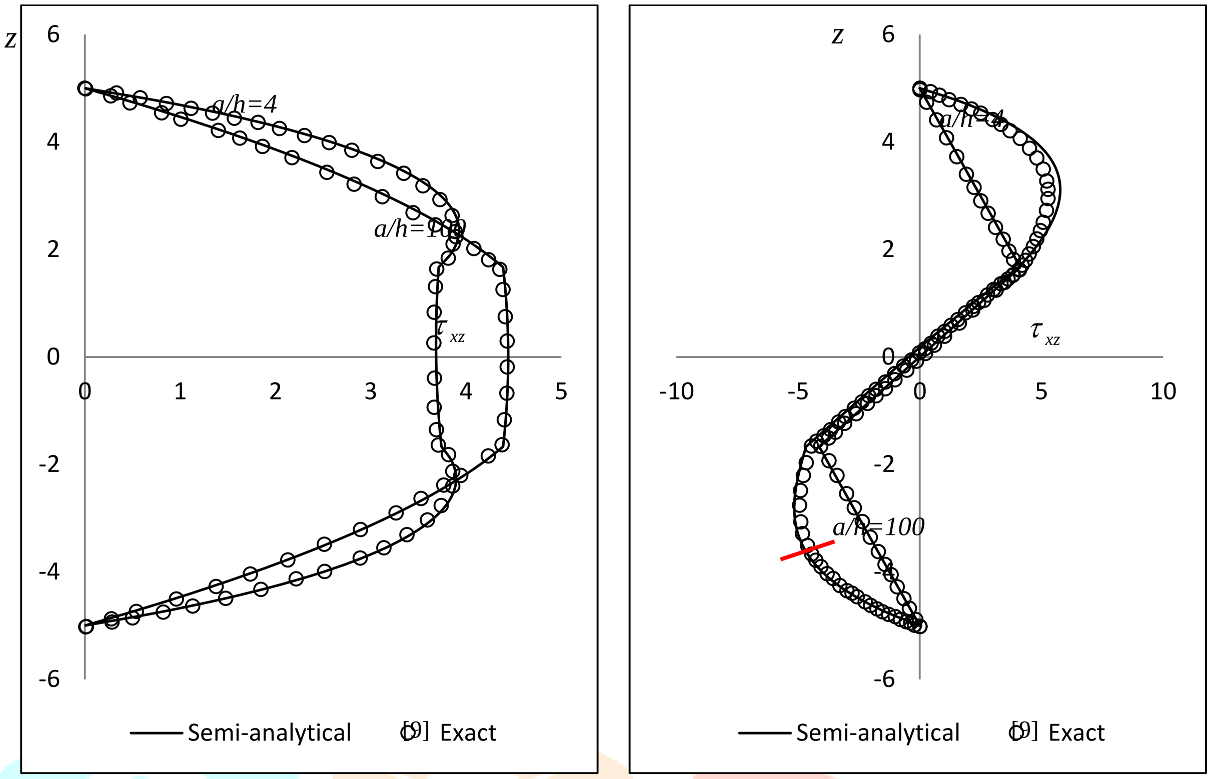

(a) (b)

Figure 8: Through thickness variation of transverse shear stress in PVDF cross ply laminate (a) applied load case, (b) applied electric potential case

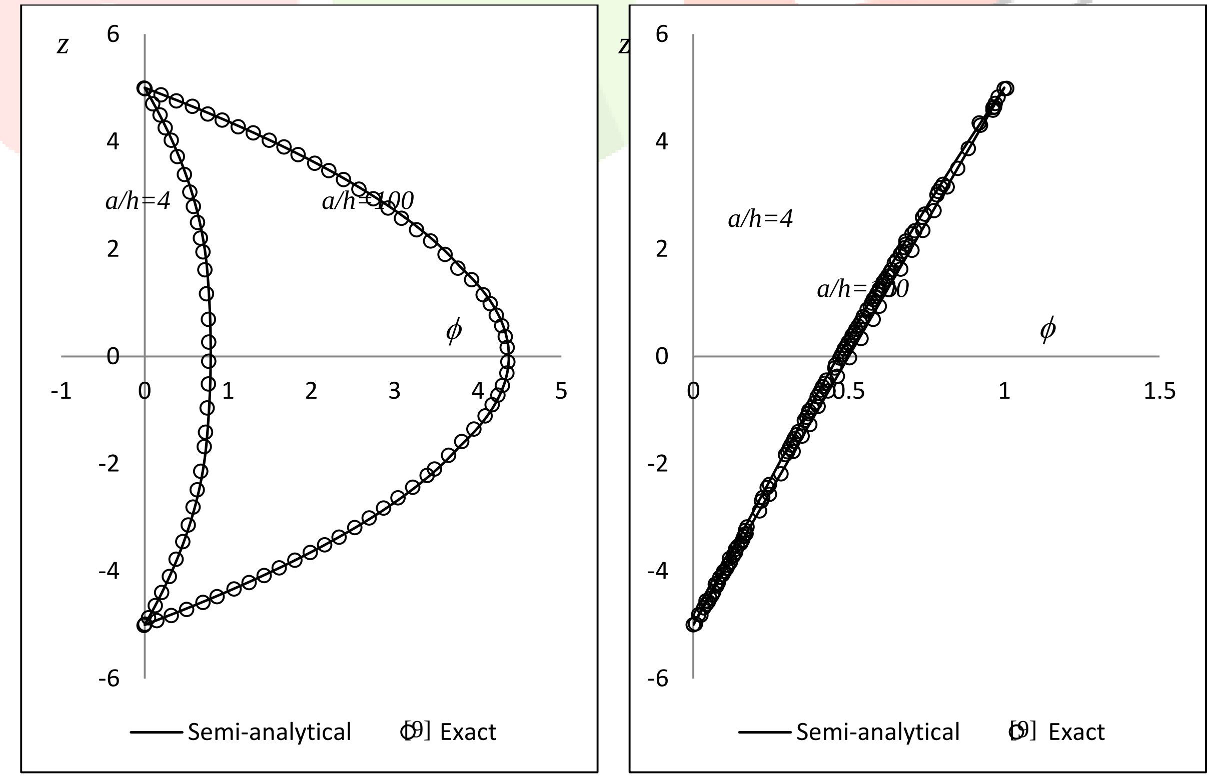

(a) (b)

Figure 9: Through thickness variation of electric potential in PVDF cross ply laminate (a) applied load case, (b) applied electric potential case

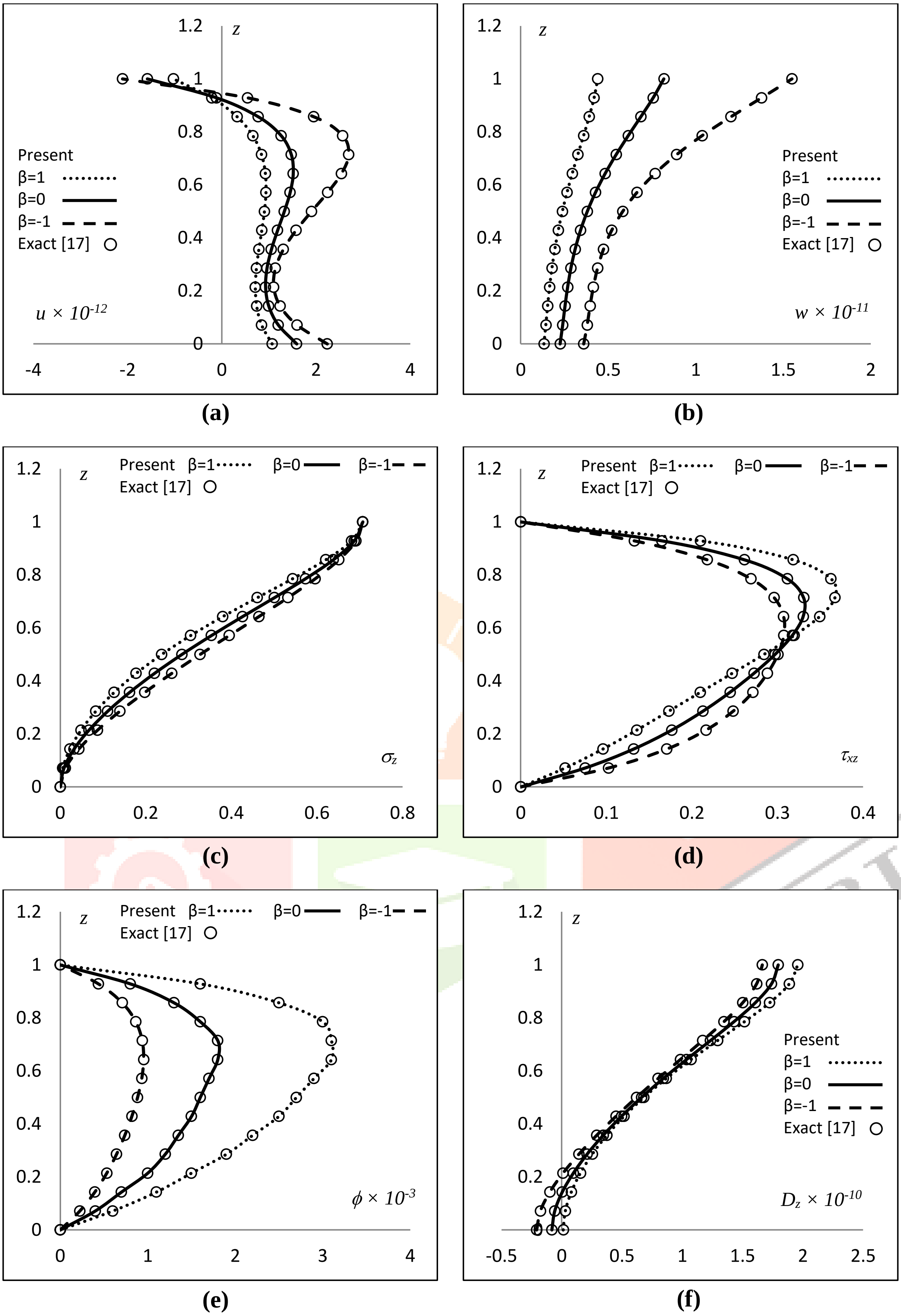

Figure 10: Through thickness variation in piezoelectric FGM plate under mechanical load in (a) in-plane displacement, (b) transverse displacement, (c) transverse normal stress, (d) transverse shear stress, (e) induced electric potential, (f) transverse electric displacement

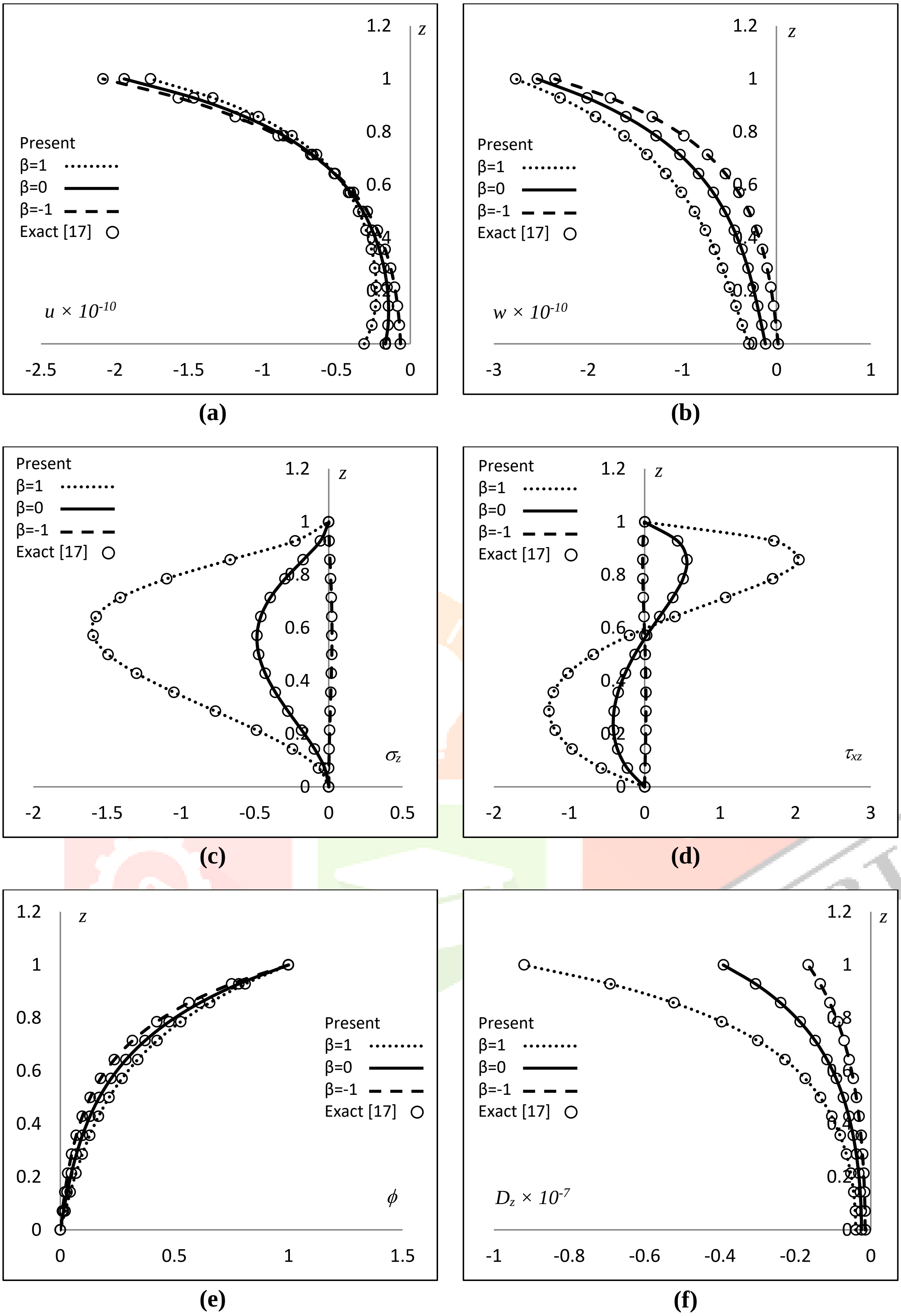

Figure 11: Through thickness variation in piezoelectric FGM plate under electric load in (a) in-plane displacement, (b) transverse displacement, (c) transverse normal stress, (d) transverse shear stress, (e) applied electric potential, (f) transverse electric displacement